Published in final edited form as:
Toxicol Pathol. 2008 ; 36(3): 397–409. doi:10.1177/0192623308315832.

Immunolocalization of Kim-1, RPA-1, and RPA-2 in Kidney of Gentamicin-, Mercury-, or Chromium-Treated Rats: Relationship to Renal Distributions of iNOS and Nitrotyrosine

Jun Zhang[1], **Ronald P. Brown**[2], **Martin Shaw**[3], **Vishal S. Vaidya**[4], **Yuzhao Zhou**[2], **Parvaneh Espandiari**[1], **Nakissa Sadrieh**[1], **Melvin Stratmeyer**[2], **Joe Keenan**[3], **Cormac G. Kilty**[3], **Joseph V. Bonventre**[4], and **Peter L. Goering**[2]

[1]Center for Drug Evaluation and Research, Food and Drug Administration, Silver Spring, Maryland, USA [2]Center for Devices and Radiological Health, Food and Drug Administration, Silver Spring, Maryland, USA [3]Biotrin International Ltd., Dublin, Ireland [4]Harvard Institutes of Medicine, Renal Division, Department of Medicine, Brigham and Women's Hospital, Harvard Medical School, Boston, Massachusetts, USA

Abstract

Immunohistochemical studies for kidney injury molecule-1 (Kim-1), renal papillary antigen-1 (RPA-1), and renal papillary antigen-2 (RPA-2) were conducted to explore their relationship to inducible nitric oxide synthase (iNOS) and nitrotyrosine expression. Male Sprague-Dawley rats were exposed to gentamicin (100 mg/kg/day Gen, sc, for 3 days), mercury (0.25 mg Hg/kg, iv, single dose), or chromium (5 mg Cr/kg, sc, single dose) and kidney tissue was examined 24 hours or 72 hours after the last dose of the nephrotoxicant. Another group of kidneys was evaluated 24 hours after rats were administered 3 daily doses (50, 100, 150, 200, or 300 mg/kg/day) of Gen. Gen- and Cr-treated rats exhibited increased immunoreactivity of Kim-1, RPA-1, and RPA-2 largely in the S1/S2 segments and to a lesser extent in the S3 segments of the proximal tubule of the kidney, whereas Hg-treated rats showed increased immunoreactivity of Kim-1, RPA-1, and RPA-2 in the S3 segments. Up-regulation of Kim-1, RPA-1, and RPA-2 expression correlated with injured tubular epithelial cells and also correlated with immunoreactivity of iNOS and nitrotyrosine. It is possible that iNOS activation with nitrotyrosine production in injured nephron segments may be involved in the induction of Kim-1, RPA-1, and RPA-2 following exposure to nephrotoxicants.

Keywords

chromium; gentamicin; Kim-1 (kidney injury molecule-1); mercury; nitrotyrosine; RPA-1 (renal papillary antigen-1); RPA-2 (renal papillary antigen-2).

Introduction

Localization of the site of injury in nephron segments has pathogenic and practical implications in the preclinical study of nephrotoxicity. Topographic histomorphology of segmental injury

Address correspondence to: Jun Zhang, MD, MS, Division of Applied Pharmacology Research, Center for Drug Evaluation and Research, Food and Drug Administration (HFD-910), 10903 New Hampshire Ave, Silver Spring, MD 20993; e-mail: jun.zhang@fda.hhs.gov..

This article was written in a personal capacity and does not represent the opinion of the Food and Drug Administration.

can help define mechanisms of toxic action and aid the search for site-specific biomarkers. The mechanisms underlying this site-selective injury are multifaceted but may be attributed in part to site-specific differences in pathophysiological properties (Schnellmann, 2001). Other factors such as animal species, age, dose regimen, treatment duration, the route of drug administration, and the choice of anesthetics may also contribute to the differences (Daugaard et al., 1987). Recent studies demonstrated that in immature and young Sprague-Dawley (SD) rats, gentamicin sulfate (Gen), an aminoglycoside antibiotic, induced renal tubular necrosis and apoptosis predominantly in the S1/S2 segments and partially in the S3 segments of the proximal tubule, whereas cisplatin, an antineoplastic agent, selectively induced necrosis and apoptosis in the S3 segment, the loop of Henle (LH), and collecting ducts (CD) of the medulla (Espandiari et al., 2007a, 2007b). In contrast to injury induced by Gen, cisplatin-induced renal injury spared most of the S1/S2 segments. Likewise, a recent study on male Wistar rats revealed that chromium (Cr; $K_2Cr_2O_7$) exclusively affected the S1/S2 segments, whereas cisplatin selectively damaged the S3 segment of the proximal tubule (Cristofori et al., 2007). In previous studies cited in the literature, most histological observations are in agreement on drug-induced segmental injury; however, it was noted that there was inconsistency in the localization of segmental injury induced by some nephrotoxicants. For example, evidence of this inconsistency can be observed in reports demonstrating that cisplatin preferentially induced histological changes in proximal tubules in adult rats and not in distal tubules and CD in 10- and 55-day-old rats (Appenroth et al., 1990), or in the S1/S2 and S3 segments in rats (Daugaard et al., 1987, 1988; Daugaard and Abildggard, 1989), or in the proximal tubules in dogs (Daugaard et al., 1987), or in the distal convoluted tubules (DCT) and CD in patients (Gonzales-Vitale et al., 1977).

Localization of the histological distribution of inducible nitric oxide synthase (iNOS) and nitrotyrosine in the nephron may have important implications for elucidating why certain nephron segments are affected by certain toxicants, but not by others, and advance the search for biomarkers of toxic injury mediated by oxidative stress. In healthy male SD rats, constitutive iNOS mRNA is expressed differentially in the various segments of the nephron. Prominent expression of iNOS was detected in the S3 segment, the thick ascending limb of LH, DCT, and the cortical and inner medullary CD, whereas much less expression of iNOS was noted in the thin limbs of LH, PCT, and the outer medullary CD (Ahn et al., 1994; Bachmann, 1997; Wu et al., 1999). In healthy male SD rats, much less nitrotyrosine immunoreactivity was seen in the epithelial cells of proximal tubules (Bian et al., 1999). Since peroxynitrite is produced by the reaction of nitrotyrosine with iNOS-derived NO, peroxynitrite formation is considered to be an important step in the development of many NO-mediated pathological processes in vivo (Forbes et al., 2002; Pacher et al., 2007).

To correlate urinary biomarkers with the site of injury in the nephron, a panel of monoclonal and polyclonal antibodies (mAbs and pAbs) specific for the recognition of antigens in specific individual tubule segments has been developed. The expression of kidney injury molecule-1 (Kim-1) by immunohistochemistry (IHC) was reported to predominate in the S3 segments in rats in models of injury where that segment is most affected (Ichimura et al., 1998,2004;Amin et al., 2004;van Timmerren et al., 2006;Vaidya et al., 2006;de Borst et al., 2007;Zhou et al., 2008) and in the S1/S2 proximal tubule segments in biopsy specimens from humans (Han et al., 2002;Zhang et al., 2008;Lin et al., 2007;van Timmerren et al., 2007; for summary, see Table 1) where there is little outer medullary tissue. New antibodies to renal papillary antigen-1 (RPA-1) and renal papillary antigen-2 (RPA-2) have been demonstrated to recognize antigens in the CD and the LH epithelial cells, respectively (Falkenberg et al., 1996;Hilderbrand et al., 1999;Shaw, 2005;Kilty et al., 2007). Thus, these new site-specific antibodies provide an opportunity to study the localization of tubular injury and may serve as robust biomarkers in preclinical and clinical studies of nephrotoxicity (Vaidya and Bonventre, 2006;Kilty et al., 2007).

The goal of the present study was to elucidate mechanisms that may trigger site-specific up-regulation of Kim-1, RPA-1, and RPA-2 and to explore morphological evidence of these proteins as biomarkers of nephrotoxicity. Specifically, we have employed rat models of Gen-, mercury (Hg)-, or Cr-induced nephrotoxicity: (a) to investigate the specific cellular distribution of Kim-1, RPA-1, and RPA-2 in different segments of the nephron using immunohistochemical methods; (b) to relate these findings to the immunohistochemical localization of iNOS and nitrotyrosine in an attempt to elucidate mechanisms possibly responsible for the up-regulation of Kim-1, RPA-1, and RPA-2; and (c) to correlate these immunoreactivities with the extent of the site-selective necrosis and apoptosis.

Materials and Methods

The experimental protocol was approved by the Institutional Animal Care and Use Committee, Center for Devices and Radiological Health, FDA, and conducted in an AAALAC (Association for Assessment & Accreditation of Laboratory Animal Care) accredited facility. All procedures for animal care and housing were in compliance with the *Guide for the Care and Use of Laboratory Animals* (National Research Council, 1996). All animals were housed in an environmentally controlled room (18–21°C, 40%-70% relative humidity) with a 12-hour light/dark cycle and were fed Certified Purina Rodent Chow and water ad libitum.

Study 1 (Time Response Study)

Adult male SD rats (10–12 weeks old, weighing 270–300 g) were purchased from Harlan (Indianapolis, IN) and divided into 9 groups. Rats in groups 1 and 2 (n = 6) each received a single sc injection of 100 mg Gen/kg daily for 3 days. Rats in groups 3 and 4 (n = 6) each received a single iv injection of 0.25 mg Hg/kg ($HgCl_2$). Rats in groups 5 and 6 (n = 6) each received a single sc injection of 5 mg Cr/kg ($K_2Cr_2O_7$). All agents were purchased from Sigma Chemical Company (St. Louis, MO). Control rats in groups 7–9 (n =3 each) were injected with saline (vehicle for Hg and Cr) or deionized water (vehicle for Gen). Rats were euthanized 24 hours or 72 hours after the single injection of Hg and Cr and 24 or 72 hours after the third and final daily dose of Gen.

Study 2 (Dose Response Study)

Rats were divided into 6 groups, with n = 6 for groups 1, 2, 3, and 6 and n = 4 for groups 4 and 5. The rats in groups 1 to 5 received a single injection of Gen daily at doses of 50, 100, 150, 200, or 300 mg/kg/day, sc, for 3 days, respectively. Control rats (n = 6) in group 6 received sc injections with dH_2O. All rats were euthanized 24 hours after the third and final daily dose of Gen.

In studies 1 and 2, kidneys were collected at necropsy and fixed in 10% zinc-formalin for about 48 hours, embedded in paraffin, cut at a thickness of 5 μm, and then stained with hemotoxylin-eosin for histopathological study. Unstained, formalin-fixed, paraffin-embedded tissue sections were used for immunohistochemical studies.

Grading System for Renal Lesions

Renal lesions were assessed by light microscopic examination in blinded fashion using a scale of 0 to 5, according to the severity of tubular cell necrosis, apoptosis, degeneration, regeneration, tubular dilatation and protein casts, glomerular vacuolization, glomerular mesangial cell proliferation, and interstitial lymphocytic infiltration in the S1/S2 segments or S3 segments: 0 = normal histology; 1 = tubular epithelial cell degeneration, without significant necrosis or apoptosis; 2–5 = <25%, <50%, <75% and ≥75% of the tubules showing tubular epithelial cell necrosis and apoptosis accompanied with other concomitant alterations, respectively.

Immunohistochemical Studies

Renal tubular epithelial cell apoptosis was detected using the TUNEL procedure, according to the manufacturer's instructions (Trevigen, Inc, Gaithersburg, MD).

For detection of Kim-1, RPA-1, and RPA-2, indirect immunoperoxidase staining procedures were used. Serial sections of formalin-fixed, paraffin-embedded renal tissue were mounted on glass slides coated with poly-L-Lysine (American HistoLabs, Inc, Gaithersburg, MD). Preparation of these sections included microwave irradiation in a pressure cooker with antigen retrieval Citra solution. After microwave treatment, slides were cooled in the antigen retrieval Citra solution for 20 minutes and then rinsed with dH_2O. For blocking endogenous peroxidase activity, sections were incubated with 0.3% hydrogen peroxide in methanol for 30 minutes and then with 5% normal horse serum for 30 minutes. Sections were incubated overnight at 4°C with the following primary mAb at 1:50 dilutions: mouse anti-rat Kim-1 ectodomain (MARKE) mAb (Harvard Medical School), RPA-1 purified mAb (Code: BI087CD, Biotrin International Ltd), and RPA-2 purified mAb (Code: BI088LH, Biotrin International Ltd). Subsequently, sections were incubated with a biotinylated secondary antibody (Vector, Burlingame, CA) for 1 hour and then incubated with avidin-biotinylated horseradish peroxidase complex (Vector) for 30 minutes. The peroxidase reaction was carried out with 0.05% 3′3′-diaminobenzidine in 0.1 M Tris-HCl buffer and 0.01% hydrogen peroxide for 10 minutes. The immunostained sections were counterstained with hematoxylin for 1 minute. For negative control staining, the primary mAb was omitted from the incubation step. The isotype mouse IgGs matched for the primary mAbs for Kim-1, RPA-1, and RPA-2 are not available from the manufacturers.

Immunoperoxidase stains for iNOS (1:100 dilution; BD Biosciences, San Diego, CA) and nitrotyrosine (1:100 dilution; Cell Sciences, Norwood, MA) were performed on 5-μm sections of formalin-fixed, paraffin-embedded tissues utilizing the avidin-biotin complex immunoperoxidase technique (Vectastain Elite kit, Vector Laboratories, Burlingame, CA) with antigen retrieval by microwave for 30 minutes in a 10 mM Citra solution. For negative controls, the primary antibodies recognizing iNOS and nitrotyrosine were omitted or replaced by the isotype-matched mouse IgG_{2a} (BD Biosciences) for iNOS and mouse IgG_{2b} (Cell Sciences) for nitrotyrosine, respectively (Zhang et al., 2006).

Statistics

A Kruskal-Wallis rank test was used to assess differences in renal lesion scores. A p value < 0.05 was considered statistically significant.

Results

Histopathology

In Gen-, Hg-, or Cr-treated rats (study 1, time response study), renal lesion scores were greater at 72 hours after the last dose (scores of 3.3, 3.8, 4.8, for Gen, Hg, and Cr, respectively) than at 24 hours (scores of 1.5, 3.0, 2.8, for Gen, Hg, and Cr, respectively) (Table 2). In the dose-response Gen study (study 2), renal lesion scores at 24 hours after the last dose increased with dose (scores of 1.2, 1.5, 2.3, 3.5, and 4.8 at doses of 50, 100, 150, 200, and 300 mg/kg, respectively) (Table 3).

In studies 1 and 2, the patterns of tubular injury were similar. Epithelial cell necrosis was more prominent in the S1/S2 segments compared to the S3 segments in Gen- or Cr-treated rats. No significant changes were seen in any segments of LH and CD in the outer and inner medulla. Epithelial cell necrosis was usually accompanied with other less severe morphological alterations: cytoplasmic vacuolization, regeneration, and hyperplasia. Vacuolization of tubular epithelial cells of the S3 segments was prevalent in Hg-treated rats, whereas epithelial

regeneration and hyperplasia of the S1/S2 and S3 segments were more evident in Gen- or Cr-treated rats.

Immunolocalization of Kim-1

Control rats exhibited no positive immunoperoxidase staining for Kim-1 in any segments of the nephron (Figure 1A), which is consistent with several published reports (Table 1). In the time course study, a positive reaction for Kim-1 was detected at the apical surface of individual cells of the S1/S2 segments 24 hours after the final injection in rats treated with Gen 100 mg/kg, sc (Figure 1B), whereas at 72 hours after the final injection, the apical positive staining became diffuse within the entire cytoplasm of tubular epithelial cells of the S1/S2 segments at sites of necrosis and apoptosis, particularly in the cytoplasm of desquamated necrotic cells in the lumen of these tubules (Figure 1C). The apical and cytoplasmic immunostaining pattern for Kim-1 was also visualized at 24 hours and at 72 hours, respectively, in Hg- (Figures 1E, 1F) or Cr-treated rats (Figures 1G, 1H).

In the dose-response study, 24 hours after the last administration of Gen injected sc for 3 days, Kim-1 immunoreactivity increased with the dose. At 24 hours after Gen 50 or 100 mg/kg, sc for 3 days, Kim-1 immunoreactivity was localized to individual S1/S2 segments. At doses of 150 and 200 mg/kg Gen, Kim-1 immunoreactivity extended to clusters of the S1/S2 segments. At the highest dose of 300 mg/kg of Gen, Kim-1 expression was localized in most of the S1/S2 segments and in a few S3 segments in the medullary rays (Figure 1D).

A lower magnification photomicrograph of a Kim-1-stained kidney section clearly showed the topographic distribution of Kim-1 expression; immunoreactivity was higher in the S1/S2 segments of the cortex but lower in the S3 segments of the outer medulla and medullary rays 72 hours posttreatment in rats injected with Gen 100 mg/kg, sc (Figure 2). A summary of time- and dose-dependent Kim-1 expression is presented in Tables 2 and 3, respectively.

Immunolocalization of RPA-1

Control rats exhibited positive immunostaining for RPA-1, which was mainly concentrated in the CD epithelial cells in the outer and inner medulla and papilla (Figure 3A) and expressed in the cytoplasm of CD cells (cover illustration). RPA-1 immunoreactivity was also diffusely localized in the cytoplasm of the cortical CD epithelial cells (Figure 3B) in control rats.

The immunostaining pattern and intensity of RPA-1 in the cortical, medullary, and papillary CD were similar between control (Figure 3A) and Gen-treated rats (Figures 3C, 3E). However, additional RPA-1 expression was noted in necrotic and apoptotic epithelial cells of the S1/S2 segments in rats 24 hours after the final of 3 daily injections of 50 mg Gen/kg (Figure 3D). In rats treated with 300 mg Gen/kg for 3 days, RPA-1 expression in the S1/S2 segments became intense (Figure 3F). A lower magnification photomicrograph showed that constitutive, basal RPA-1 expression in the cortical CD cells coexisted with nascent RPA-1 in the S1/S2 segments of the cortex and in the S3 segments of the outer medulla in rats 72 hours after the final of 3 daily injections of 100 mg Gen/kg, sc (Figure 2).

In Hg-treated rats, RPA-1 expression was observed in the S3 segments 24 hours posttreatment (Figure 3G). In contrast, in Cr-treated rats, RPA-1 immunoreactivity was expressed in the S1/S2 segments 24 hours posttreatment (Figure 3H).

Immunolocalization of RPA-2

Control rats exhibited a robust basal level of RPA-2 expression in the medullary LH (Figure 4A). The immunoperoxidase staining for RPA-2 in control rats showed cytoplasmic localization in the epithelial cells of the descending and ascending thin LH segments in the

medulla (Figure 4B). RPA-2 expression was sporadically located in the epithelial cells of thick ascending LH in the cortex (Figure 4C). No significant visible differences of RPA-2 immunoreactivity were apparent in medullary LH cells between control (Figure 4A) and Gen-treated rats (Figure 4D). In contrast, in addition to the high basal expression of RPA-2 in the epithelial cells in the ascending thick LH segments of the cortex, nascent RPA-2 expression appeared in the proximal tubules (Figure 2) in Gen-treated rats. In higher magnification photomicrographs in Gen-treated rats, RPA-2 expression was observed in the S1/S2 segments (Figures 4E, 4F) adjacent to LH segments. The immunostaining intensity in the S1/S2 segments was stronger at 24 hours than at 72 hours after completion of 3 Gen injections, and the cytoplasmic coarse granules at 24 hours (Figure 4E) became a weaker and homogenous cytoplasmic stain after 72 hours posttreatment (Figure 4F).

In Hg-treated rats, RPA-2 expression was not increased above basal levels in the cortical LH epithelial cells (Figure 4G) and no RPA-2 was detected in the S1/S2 segments. In Cr-treated rats, basal RPA-2 expression was localized to the cortical LH epithelial cells; however, in contrast to Hg treatment, RPA-2 expression was also observed in the S1/S2 segments (Figure 4H).

Immunolocalization of Apoptosis, iNOS, and Nitrotyrosine

No apoptotic cells and no expression of iNOS or nitrotyrosine were found in the cortex and medulla in control rats (Figures 5A-5C). However, in Gen- and Cr-treated rats, a significant number of apoptotic cells were detected in the epithelia of the S1/S2 segments (Figures 5D, 5J), whereas in Hg-treated rats, apoptotic cells were located in S3 tubular cells (Figure 5G). The expression of iNOS was apparent in S1/S2 segments and in S3 segments (Figure 5E) in Gen-treated rats, in S3 segments in Hg-treated rats (Figure 5H), and in the S1/S2 segments in Cr-treated rats (Figure 5K). Nitrotyrosine expression was up-regulated in the S1/S2 segments and a few S3 segments in Gen-treated rats (Figure 5F), in the S3 segments in Hg-treated rats (Figure 5I), and in the S1/S2 segments and a few S3 segments in Cr-treated rats (Figure 5L).

Discussion

The present study has provided some new and interesting information regarding the immunolocalization of Kim-1, RPA-1, and RPA-2 in response to nephrotoxicants. The data will provide a critical basis to generate hypotheses for future studies.

Increased Immunoreactivity of Kim-1, RPA-1, and RPA-2 in Necrotic and Apoptotic Proximal Tubular Cells

The present study demonstrated that in Gen-, Hg-, and Cr-treated rats, Kim-1 immunoreactivity increased significantly compared to that of control kidneys. Kim-1 immunoreactivity correlated well with the severity of tubular epithelial cell necrosis and apoptosis, and the increases in Kim-1 immunoreactivity were time and dose dependent. For Gen and Cr exposures, Kim-1 immunoreactivity was observed to be predominantly localized in the S1/S2 segments and less markedly in the S3 segments. In contrast, for Hg exposure, Kim-1 immunoreactivity was observed predominately in the S3 segments, which are the primary targets where mercuric ions accumulate and express toxicity after exposure to elemental or inorganic forms of Hg (Diamond and Zalups, 1998). For all 3 nephrotoxicants, Kim-1 did not appear to be localized in any other nephron segments, that is, CD or LH. These findings are consistent with previous observations of undetectable Kim-1 in normal healthy kidneys, and its marked increase under pathological conditions (Amin et al., 2004; de Borst et al., 2007; Han et al., 2002; Ichimura et al., 1998, 2004; Lin et al., 2007; Vaidya et al., 2006; van Timmerren et al., 2006, 2007; Vaidya and Bonventre, 2006; Zhou et al., 2008).

Interestingly, RPA-1 and RPA-2 immunoreactivity above constitutive levels was also detected in Gen-, Hg-, and Cr-treated rats. Differences in RPA-1 and RPA-2 immunolocalization were also observed between rats treated with Gen or Cr (the S1/S2 segments, or the S3 segments) and rats treated with Hg (the S3 segments). An explanation for why Gen, Hg, and Cr induced different immunolocalization of Kim-1, RPA-1, and RPA-2 is unknown.

Immunoreactivity of RPA-1 and RPA-2 in CD and LH

In control and all rats treated with nephrotoxicants, no Kim-1 immunoreactivity was identified in the CD and LH of the medulla and papilla. The negative immunoreactivity of Kim-1 in the LH and CD highlights its specificity as a biomarker of proximal tubular epithelial cell injury. In contrast, RPA-1 and RPA-2 immunoreactivity was detected in the CD and LH, respectively, in the cortex, medulla, and papilla from control and all treated rats. The localization of RPA-1 in the medulla and cortex is consistent with previous observations (Falkenberg et al., 1996). Moreover, the immunoreactivity patterns of RPA-1 and RPA-2 were similar in both control and all treated rats. These findings were consistent with the expected results, because no histopathologic injury in the medulla and papilla was observed in any treated rats.

Relation of the Site Predilection of Kim-1, RPA-1, and RPA-2 to Renal Distribution of iNOS and Nitrotyrosine

Little or no Kim-1 mRNA and Kim-1 protein is expressed in the proximal tubular epithelial cells of the normal adult rat kidney; however, a variety of pathological conditions in the kidney up-regulate its expression (Ichimura et al., 1998,2004;Vaidya and Bonventre, 2006; van Timmerren et al., 2006,2007;Kramer et al., 2007;Zhou et al., 2008). In contrast, little is known about mRNA and proteins of RPA-1 and RPA-2 in normal and injured cells of the S1/S2 segments. In the present study, necrotic and apoptotic cells of the S1/S2 and S3 segments were immunoreactive to Kim-1, RPA-1, and RPA-2, but normal epithelial cells of these segments were not. Moreover, the same sites of predilection were also immunoreactive for iNOS and nitrotyrosine antigens. These findings suggest that the intracellular, immunoreactive Kim-1, RPA-1, and RPA-2 proteins were more abundant in injured, necrotic, and apoptotic cells of the S1/S2 and S3 segments than in their normal healthy counterparts. Kim-1, RPA-1, and RPA-2 immunoreactivities appear to be enhanced in nephron locations where iNOS and nitrotyrosine immunoreactivities are increased. Whether increased immunoreactive proteins represent enhanced de novo protein synthesis of RPA-1 and RPA-2 or reduced degradation of constitutive protein remains to be determined. Kim-1 mRNA is not expressed in healthy cells, and the cellular processes responsible for enhanced Kim-1 expression after nephrotoxicant administration are not entirely known.

Up-Regulation of Peroxynitrite as a Potential Mechanism of Renal Injury

Many renal pathological conditions, for example, ischemia/reperfusion injury with or without endotoxin insult and diabetic nephropathy, can significantly promote NO production and peroxynitrite formation. There have been several reports concerning the beneficial or detrimental effects of NO on renal injury. It was suggested that NO formation prevents Gen-induced nephrotoxicity in a model of rat acute renal failure (Ghaznavi et al., 2005) and that iNOS contributes to the prolonged protective effects of ischemic preconditioning in the mouse kidney (Park et al., 2003). In contrast, iNOS gene knockout mice are protected against hypoxic injury in renal proximal tubules (Ling et al., 1998). At present, it is difficult to reconcile these disparate findings involving opposite effects of iNOS; however, the concept of an initial beneficial and late detrimental effect seems reasonable and acceptable as an explanation (Amin et al., 2004).

In this context, the present study is consistent with the reported cytotoxic effects of NO generated from iNOS on acute tubular necrosis and apoptosis in Gen-, Hg-, and Cr-induced

nephrotoxicity (Kim et al., 1997; Yanagisawa et al., 1998; Baliga et al., 1999; Bagchi et al., 2001; Basnakian et al., 2002; Maldonado et al., 2003; Pedraza-Chaverri et al., 2005; Parlakpinar et al., 2005). Furthermore, it was reported that NO results in oxidative damage and contributes to the "point of no return" of host cell injury, necrosis, and apoptosis (Thuraisingham et al., 2000; Goligorsky et al., 2002; Yokozawa et al., 2002; Forbes et al., 2002; Nakajima et al., 2006; Pacher et al., 2007). A recent review suggests that NO does not have as many potential toxic effects as previously reported. Most of the cytotoxicity attributed to NO is rather due to the peroxynitrite and peroxynitrite anion, which is more reactive and toxic than NO (Pacher et al., 2007). Peroxynitrite is capable of causing protein tyrosine nitration (Radi, 2004) and is also capable of mediating damage in renal mitochondria and apoptosis (Yokozawa et al., 2002). Radi (2004) suggested that peroxynitrite can cause protein tyrosine nitration in vitro and in vivo. NO does not directly produce nitrotyrosine, but it reacts rapidly with superoxide anion and forms peroxynitrite, a potent nitrating and oxidizing agent (Kim et al., 1997). Peroxynitrite can induce oxidative damage to proteins, DNA, and lipids (Bian et al., 1999; Schnellmann, 2001). Nitrotyrosine can be detected immunohistochemically using an antibody against nitrotyrosine (Bosse and Bachmann, 1997). Immunohistochemical localization of nitrotyrosine in the proximal tubular epithelial cells was detected in Gen-treated rats (Maldonado et al., 2003). Enhanced expression of nitrotyrosine correlated with necrotic tubular cells in Cr-treated rats (Pedraza-Chaverri et al., 2005). Recent reports suggest that nitrotyrosine represents the nitration of protein-bound tyrosine residues by peroxynitrite (Forbes et al., 2002) and that nitrotyrosine can be used as a marker for endogenous production of peroxynitrite (Maldonado et al., 2003).

Kim-1: A Possible Link to the Reaction of Peroxynitrite with Cysteine

Kim-1 is a type 1 membrane protein containing a 6-cysteine immunoglobulin (Ig)-like domain. Kim-1 is different from other members of the Ig superfamily in containing 6 cysteines, compared with 2 cysteines in most members of the Ig superfamily and 4 in mucosal dressin cell adhesion molecule-1 (MAdCAM-1); however, the reason for the large number of cysteines remains unclear. Kim-1 is labeled as a so-called novel Ig domain (Ichimura et al., 1998). A recent review suggests that peroxynitrite reacts with various amino acids (Pacher et al., 2007). Of these reactions, that of peroxynitrite with cysteine is the most prevalent. In addition, cysteine oxidation by peroxynitrite can promote enzyme activation and modify proteins (Pacher et al., 2007). Based on these findings, we hypothesize that the reaction of peroxynitrite and cysteine may lead to alterations of Kim-1 primary sequence and function. It is tempting to consider the possibility of S-nitrosylation of cysteine thiol residues, a posttranslation protein modification by the covalent addition of a nitrogen monoxide group to the thiol side chain of a protein or peptide cysteine residue (Fukumura et al., 2006). S-nitrosylation is used in mammalian cells to convey several specific signals that are elicited by NO (Fukumura et al., 2006). Further studies are needed to evaluate this hypothesis.

Spatial Relationship between the Apical Location of Kim-1 and the Subapical Location of Nitrotyrosine

In endotoxin-treated rats, enhanced immunoreactivity of nitrotyrosine was attributed to reabsorption of hydrolytic nitrated proteins by proximal tubule epithelial cells (Bian et al., 1999). The marked staining of nitrotyrosine in proximal epithelial cells was in the subapical compartment where the endocytic lysosomes are located (Bian et al., 1999). A key finding is that nitrotyrosine is located at the apical cytoplasm beneath the luminal brush border of the S1/S2 segments (Bian et al., 1999). Similarly, immunohistochemical staining for renal nitrotyrosine in experimental diabetic nephropathy revealed that nitrotyrosine was mostly localized to the apical region of proximal tubular cells (Forbes et al., 2002). The present and previous studies (Han et al., 2002; Ichimura et al., 1998, 2004; Lin et al., 2007; Vaidya et al., 2006; van Timmerren et al., 2006, 2007; Vaidya and Bonventre, 2006; Zhou et al., 2008) have

localized Kim-1 at the apical membrane of epithelial cells of proximal tubule segments. There appears to be a spatial relationship between the site-specific nitrosative injury at the subapical location and Kim-1 immunoreactivity.

Kim-1, RPA-1, and RPA-2: Potential Tissue Markers for Tubular Cell Injury

Previous studies in the laboratory have demonstrated that urinary Kim-1 is a sensitive nephrotoxicity biomarker in Gen-, Hg-, and Cr-treated rats (Zhou et al., 2008) and that urinary RPA-1 is a nephrotoxicity biomarker in Gen-treated rat (Shaw et al., 2007). Whether Kim-1, RPA-1, and RPA-2 could be used as sensitive, specific, and reliable tissue markers remains to be assessed in detail using IHC compared with the gold standard of histopathologic evaluation of hematoxylin and eosin-stained sections (Gillett et al., 2002). Previous IHC studies have demonstrated that the negative findings for RPA-1 and RPA-2 induction with proximal tubular toxicants reinforce their potential use as biomarkers for renal papillary injury and as negative controls for proximal tubular injury (Falkenberg et al., 1996; Hilderbrand et al., 1999; Shaw, 2005; Kilty et al., 2007). In the present study, induction of RPA-1 and RPA-2 in proximal tubular cells is unusual and warrants further study.

Control experiments with isotype-matched control antibodies on a serial section are important (Gillett et al., 2002). At present, these immunoglobulins are not commercially available. To compensate for the lack of these sera, immunostaining for Kim-1, RPA-1, and RPA-2 has been performed in a study using a non-nephrotoxic agent. SD rats (10-, 25-, 40-, 80-day-old) treated with valproic acid (a hepatotoxic agent) were used as animal experimental controls and compared with Gen-treated rats. No tubular epithelial injury of the kidney was found, nor was any positive reaction of Kim-1, RPA-1, and RPA-2 in renal tissues obtained from valproic acid —treated rats, compared to the positive immunostaining for these markers detected in the kidney of Gen-treated rats (manuscript, in preparation). In the present study, omission of primary antibodies of Kim-1, RPA-1, and RPA-2 resulted in a negative reaction in renal tissue sections obtained from Gen-, Hg-, and Cr-treated rats. Furthermore, no immunostaining for Kim-1, RPA-1, and RPA-2 was found in any of the proximal epithelial cells and glomerular cells in the kidney from vehicle-treated rats (Figures 1A, 3B, 4C).

Summary

The present study demonstrated that Kim-1, RPA-1, and RPA-2 are induced in the kidney, but with different immunolocalization, in Gen-, Cr-, and Hg-treated rats. The spatial relationship between expression of Kim-1, RPA-1, RPA-2, and expression of iNOS and nitrotyrosine suggests that peroxynitrite-mediated oxidative pathways may be involved in the renal injury induced by these nephrotoxicants.

Acknowledgments

The authors thank Ms. Jacintha Tolson for assistance with animal injections and necropsies. This project was supported with funds provided by the U.S. Food and Drug Administration; an appointment to the Research Fellowship Program administered by the Oak Ridge Associated Universities through a contract with the U.S. Food and Drug Administration (YZ); by NIH Grants DK-039773, DK-072831, and DK-074099 (JVB); and a Scientist Development Grant 0535492T from the American Heart Association (VSV).

Abbreviations

CD, collecting ducts
Cr, chromium ($K_2Cr_2O_7$)
DCT, distal convoluted tubule
Gen, gentamicin sulfate
Hg, mercury ($HgCl_2$)

iNOS, inducible nitric oxide synthase
Kim-1, kidney injury molecule-1
LH, loop of Henle
mAb, monoclonal antibody
NO, nitric oxide
pAb, polyclonal antibody
RPA-1, renal papillary antigen-1
RPA-2, renal papillary antigen-2
S1/S2 segments and S3 segment, the S1 & S2 segments of proximal convoluted tubules and the S3 segment of proximal straight tubule.

References

Ahn KY, Mohaupt MG, Madsen KM, Kone BC. In situ hybridization localization of mRNA encoding inducible nitric oxide synthase in the rat kidney. Am J Physiol 1994;267:F748–57. [PubMed: 7526707]

Amin RP, Vickers AE, Sistare F, Thompson KL, Roman RJ, Lawton M, Kramer J, Hamadeh HK, Collins J, Grissom S, Bennett L, Tucker CJ, Wild S, Kind C, Oreffo V, Davis JW II, Curtiss S, Naciff JM, Cunningham M, Tennant R, Stevens J, Car B, Bertram TA, Afshart CA. Identification of putative gene based markers of renal toxicity. Environ Health Perspect 2004;112:465–79. [PubMed: 15033597]

Appenroth D, Gambaryan S, Gerhardt S, Kersten L, Braunlich H. Age dependent differences in the functional and morphological impairment of kidney following cisplatin administration. Exp Pathol 1990;38:231–9. [PubMed: 2387365]

Bachmann, S. Distribution of NOS in the kidney. In: Goligorsky, MS.; Gross, SS., editors. Nitric Oxide and the Kidney: Physiology and Pathophysiology. Chapman and Hall; New York: 1997. p. 133-57.

Bagchi D, Bagchi M, Stohs SJ. Chromium (VI)-induced oxidative stress, apoptotic cell death and modulation of p53 tumor suppressor gene. Mol Cell Biochem 2001;222:149–58. [PubMed: 11678597]

Baliga R, Ueda N, Walker PD, Shah SV. Oxidant mechanisms in toxic acute renal failure. *Drug Metab* Rev 1999;31:971–97. [PubMed: 10575556]

Basnakian AG, Kaushal GP, Shah SV. Apoptotic pathways of oxidative damage to renal tubular epithelial cells. Antioxid Redox Signal 2002;4:915–24. [PubMed: 12573140]

Bian K, Davis K, Kuret J, Binder L, Murad F. Nitrotyrosine formation with endotoxin-induced kidney injury detected by immunohistochemistry. Am J Physiol 1999;277:F33–40. [PubMed: 10409295]

Bosse HM, Bachmann S. Immunohistochemically detected protein nitration indicates sites of renal nitric oxide release in Goldblatt hypertension. Hypertension 1997;30:948–52. [PubMed: 9336398]

Cristofori P, Zanetti E, Fregona D, Piaia A, Trevisan A. Renal proximal tubule segment-specific nephrotoxicity: an overview on biomarkers and histopathology. Toxicol Pathol 2007;35:270–5. [PubMed: 17366321]

Daugaard G, Abildggard U. Cisplatin nephrotoxicity. Cancer Chemother Pharmacol 1989;25:1–9. [PubMed: 2686850]

Daugaard G, Abildggard U, Larsen S, Holstein-Rathlou NH, Amtorp O, Olesen HP, Leyssac PP. Functional and histopathological changes in dog kidney after administration of cisplatin. Renal Physiol 1987;10:54–64. [PubMed: 3685614]

Daugaard G, Holstein-Rathlou NH, Leyssac PP. Effect of cisplatin on proximal convoluted and straight segments of the rat kidney. J Pharmacol Exp Ther 1988;224:1081–5. [PubMed: 3252023]

de Borst MH, van Timmeren MM, Vaidya VS, de Boer RA, van Dalen MBA, Kramer AB, Schuurs TA, Bonventre JV, Navis G, van Goor H. Induction of kidney injury molecule-1 in homozygous Ren2 rats is attenuated by blockage of the rennin-angiotensin system or p38 MAP kinase. Am J Physiol Renal Physiol 2007;292:F313–20. [PubMed: 16896183]

Diamond GL, Zalups RK. Understanding renal toxicity of heavy metals. Toxicol Pathol 1998;26(1):92–103. [PubMed: 9502391]

Espandiari P, Zhang J, Rosenzweig BA, Vaidya VS, Sun J, Schnackenberg L, Herman EH, Knapton A, Bonventre JV, Beger RD, Thompson KL, Hanig J. The utility of a rodent model in detecting pediatric drug-induced nephrotoxicity. Toxicol Sci 2007a;99:637–48. [PubMed: 17636248]

Espandiari, P.; Zhang, J.; Rosenzweig, B.; Zhou, Y.; Vaidya, VS.; Herman, EH.; Miller, TJ.; Knapton, A.; Honchel, R.; Weaver, J.; Noory, L.; Adeyemo, O.; Benedick, M.; Goering, P.; Brown, R.; Bonventre, JV.; Thompson, K.; Sadrieh, N.; Hanig, J. Age-related differences in susceptibility to cisplatin-induced renal toxicity. International Congress of Toxicity; Montreal, Canada. July 15-19; 2007b.

Falkenberg FW, Hilderbrand H, Lutte L, Schwengberg S, Henke B, Greshake D, Schmidt B, Friederich A, Rinke M, Schluter G, Bombard E. Urinary antigens as markers of papillary toxicity. I: Identification and characterization of rat kidney papillary antigens with monoclonal antibodies. Arch Toxicol 1996;71:80–92. [PubMed: 9010589]

Forbes JM, Gooper ME, Thallas V, Burns WC, Thomas MC, Bramma GC, Lee F, Grant SL, Burrell LA, Jerums G, Osicka TM. Reduction of the accumulation of advanced glycation end products by ACE inhibition in experimental diabetic nephrotoxicity. Diabetes 2002;51:3274–82. [PubMed: 12401719]

Fukumura D, Kashiwagi S, Jain RK. The role of nitric oxide in tumor progression. Cancer 2006;6:521–34. [PubMed: 16794635]

Ghaznavi R, Faghihi M, Kadkhodaee M, Shams S, Khastar H. Effects of nitric oxide on gentamicin toxicity in isolated perfused rat kidney. J Nephrol 2005;18:548–52. [PubMed: 16299680]

Gillett, N.; Chan, C.; Farman, C.; Lappin, P. Specific techniques in toxicologic pathology. In: Haschek, WM.; Rousseaux, CG.; Wallig, MA., editors. Handbook of Toxicologic Pathology. Vol. 2nd ed.. Vol. Vol. 1. Academic Press; San Diego: 2002. p. 207-41.

Goligorsky MS, Brodsky SV, Noiri E. Nitric oxide in acute renal failure: NOS versus NOS. Kidney Int 2002;61:855–61. [PubMed: 11849438]

Gonzales-Vitale JC, Hayes DM, Cvitkovic E, Sternberg SS. The renal pathology in clinical trials of *cis*-platinum (II) diammenedichride. Cancer 1977;39:1362–71. [PubMed: 851939]

Han WK, Bailly V, Abichandani R, Thadhani R, Bonventre JV. Kidney injury molecule-1 (KMI-1): a novel biomarker for human renal proximal tubule injury. Kidney Int 2002;62:237–44. [PubMed: 12081583]

Hilderbrand H, Rinke M, Schluter G, Bomhard E, Falkenberg FW. Urinary antigens as markers of papillary toxicity. II: Application of monoclonal antibodies for the determination of papillary antigens in rat urine. Arch Toxicol 1999;73:233–45. [PubMed: 10463389]

Ichimura T, Bonventre JV, Bailly V, Wei H, Hession CA, Cate RL, Sanicola M. Kidney injury molecule-1 (KIM-1), a putative epithelial cell adhesion molecule containing a novel immunoglobulin domain, is up-regulated in renal cells after injury. J Biol Chem 1998;273:4135–42. [PubMed: 9461608]

Ichimura T, Hung CC, Yang SA, Stevens JL, Bonventre J. Kidney injury molecule-1: a tissue and urinary biomarker for nephrotoxicant-induced renal injury. Am J Physiol Renal Physiol 2004;286:F552–63. [PubMed: 14600030]

Kilty CG, Keenan J, Shaw M. Histologically defined biomarkers in toxicology. Expert Opin Drug Saf 2007;6:207–15. [PubMed: 17367267]

Kim, YM.; Tzeng, E.; Billiard, TR. Role of NO and nitrogen intermediates in regulation of cell functions. In: Goligorsky, MS.; Gross, SS., editors. Nitric Oxide and the Kidney: Physiology and Pathophysiology. Chapman and Hall; New York: 1997. p. 22-51.

Kramer AB, van der Meulen EF, Hamming I, van Goor H, Navis G. Effect of combining ACE inhibition with aldosterone blockade on proteinuria and renal damage in experimental nephrosis. Kidney Int 2007;71:417–24. [PubMed: 17213874]

Kuehn EW, Park KM, Somio S, Bonventre JV. Kidney injury molecule-1 expression in murine polycystic kidney disease. Am J Physiol Renal Physiol 2002;283:F1326–36. [PubMed: 12388382]

Lin F, Zhang PL, Yang XJ, Shi J, Blasick T, Han WK, Wang HL, Shen SS, The BT, Bonventre JV. Human kidney injury molecule-1 (hKIM-1): a useful immunohistochemical marker for diagnosing renal cell carcinoma and ovarian clear cell carcinoma. Am J Surg Pathol 2007;31:371–81. [PubMed: 17325478]

Ling H, Gengaro PE, Edelstein CL, Martin P-Y, Wangsiripaisan A, Nemenoff R, Schrier RW. Effect of hypoxia on proximal tubules isolated from nitric oxide synthase knockout mice. Kidney Int 1998;53:1642–6. [PubMed: 9607195]

Maldonado PD, Barrera D, Medina-Campos ON, Hernandez-Pando R, Ibarra-Rubio ME, Pedraza-Chaverri J. Aged garlic extract attenuates gentamicin induced renal damage and oxidative stress in rats. Life Sci 2003;73:2543–56. [PubMed: 12967679]

Nakajima A, Ueda K, Takaoka M, Yoshimi Y, Matsumura Y. Opposite effects of pre- and postischemic treatments with nitric oxide donor on ischemia/reperfusion-induced renal injury. J Pharmacol Exp Ther 2006;316:1038–46. [PubMed: 16306274]

National Research Council. Guide for the Care and Use of Laboratory Animals. National Academy Press; Washington, DC: 1996.

Pacher P, Beckman JS, Liaudet L. Nitric oxide and peroxynitrite in health and disease. Physiol Rev 2007;87:315–424. [PubMed: 17237348]

Park KM, Byun J-Y, Kramers C, Kim JI, Huang PL, Bonventre JV. Induction nitric-oxide synthase is an important contributor to prolonged protective effects of ischemic preconditioning in the mouse kidney. J Biol Chem 2003;278:27256–66. [PubMed: 12682064]

Parlakpinar H, Tasdemir S, Polat A, Bay-Karabulut A, Vardi N, Ucar M, Acet A. Protective role of caffeic acid phenethyl ester (cape) on gentamicin-induced acute renal toxicity in rats. Toxicology 2005;207:167–77.

Pedraza-Chaverri J, Barrera D, Medina-Campos ON, Carvajal RC, Hernandez-Pando R, Macias-Ruvalcaba NA, Maldonado PD, Salcedo MI, Tapia E, Saldivar L, Castilla ME, Ibarra-Rubio ME. Time course study of oxidative and nitrosative stress and antioxidative enzymes in $K_2Cr_2O_7$-induced nephrotoxicity. BMC Nephrol 2005;6:4. [PubMed: 15854231]

Radi R. Nitric oxide, oxidants, and protein tyrosine nitration. Proc Natl Acad Sci U S A 2004;101:4003–8. [PubMed: 15020765]

Schnellmann, RG. Toxic response of the kidney. In: Klaassen, CD., editor. Casarett & Doull's Toxicology: The Basic Science of Poisons. Vol. 6th ed. McGraw-Hall; New York: 2001. p. 491-514.

Shaw M. The use of histologically defined specific biomarkers in drug development with special reference to the glutathione-S-transferases. Cancer Biomarkers 2005;1:69–74. [PubMed: 17192033]

Shaw M, Vaidya V, Zhou Y, Ferguson M, Zhang J, Brown R, Keenan J, Bonventre J, Goering P. Alpha-GST, GST-YB1, renal papillary antigen-1 (RPA-1) and kidney injury molecule-1 (Kim-1) are sensitive biomarkers of subclinical renal injury in gentamicin-treated rats. Toxicologist. 2007Abstract No. 464, 2007

Thuraisingham RC, Nott CA, Dodd SM, Yaqoon MM. Increased nitrotyrosine staining in kidney from patients with diabetic nephropathy. Kidney Int 2000;57:1968–72. [PubMed: 10792615]

Vaidya VS, Bonventre JV. Mechanistic biomarkers for cytotoxic acute kidney injury. Expert Opin Drug Metab Toxicol 2006;2:697–713. [PubMed: 17014390]

Vaidya VS, Ramirez V, Ichimura T, Bobadilla NA, Bonventre JV. Urinary kidney injury molecule-1: a sensitive quantitative biomarker for early detection of kidney tubular injury. Am J Physiol Renal Physiol 2006;290:F517–29. [PubMed: 16174863]

van Timmerren MM, Bakker SJL, Vaidya VS, Bailly V, Schuurs TA, Damman J, Stegeman CA, Bonventre JV, van Goor H. Tubular kidney injury molecule-1 in protein-overload nephropathy. Am J Physiol Renal Physiol 2006;291:F456–64. [PubMed: 16467126]

van Timmerren MM, van den Heuvel MC, Bailly V, Bakker SJL, van Goor H, Stegeman CA. Tubular kidney injury molecule-1 in human renal disease. J Pathol 2007;212:209–17. [PubMed: 17471468]

Wu F, Park F, Cowley AW Jr. Mattson DL. Quantification of nitric oxide synthase activity in microdissected segments of the rat kidney. Am J Physiol 1999;276:F874–81. [PubMed: 10362776]

Yanagisawa H, Nodera M, Wada O. Inducible nitric oxide synthase expression in mercury chloride-induced acute tubular necrosis. Ind Health 1998;36:324–30. [PubMed: 9810145]

Yokozawa T, Chen CP, Rhyu DY, Tanaka T, Park JC, Kitani K. Potential of sanguiin H-6 against oxidative damage in renal mitochondria and apoptosis mediated by peroxynitrite in vivo. Nephron 2002;92:133–41. [PubMed: 12187096]

Zhang J, Herman EH, Robertson DG, Reily MD, Knapton A, Ratajczak HV, Rifai N, Honchel R, Blanchard KT, Stoll RE, Sistare FD. Mechanisms and biomarkers of cardiovascular injury induced by phosphodiesterase inhibitor III SK&F 95654 in the spontaneously hypertensive rat. Toxicol Pathol 2006;34:152–63. [PubMed: 16537294]

Zhang PL, Rothblum LI, Han WK, Blasick TM, Potdar S, Bonventre JV. Kidney injury molecule-1 expression in proximal tubules of renal transplant biopsies is a sensitive measure of proximal tubular cell injury. Kidney Int 2008;73(5):608–14. [PubMed: 18160964]

Zhou Y, Vaidya VS, Brown RP, Zhang J, Rosenzweig BA, Thompson KL, Miller T,J, Bonventre JV, Goering PL. Comparison of kidney injury molecule-1 and other nephrotoxicity biomarkers in urine and kidney following acute exposure to gentamicin, mercury, and chromium. Toxicol Sci 2008;101:159–70. [PubMed: 17934191]

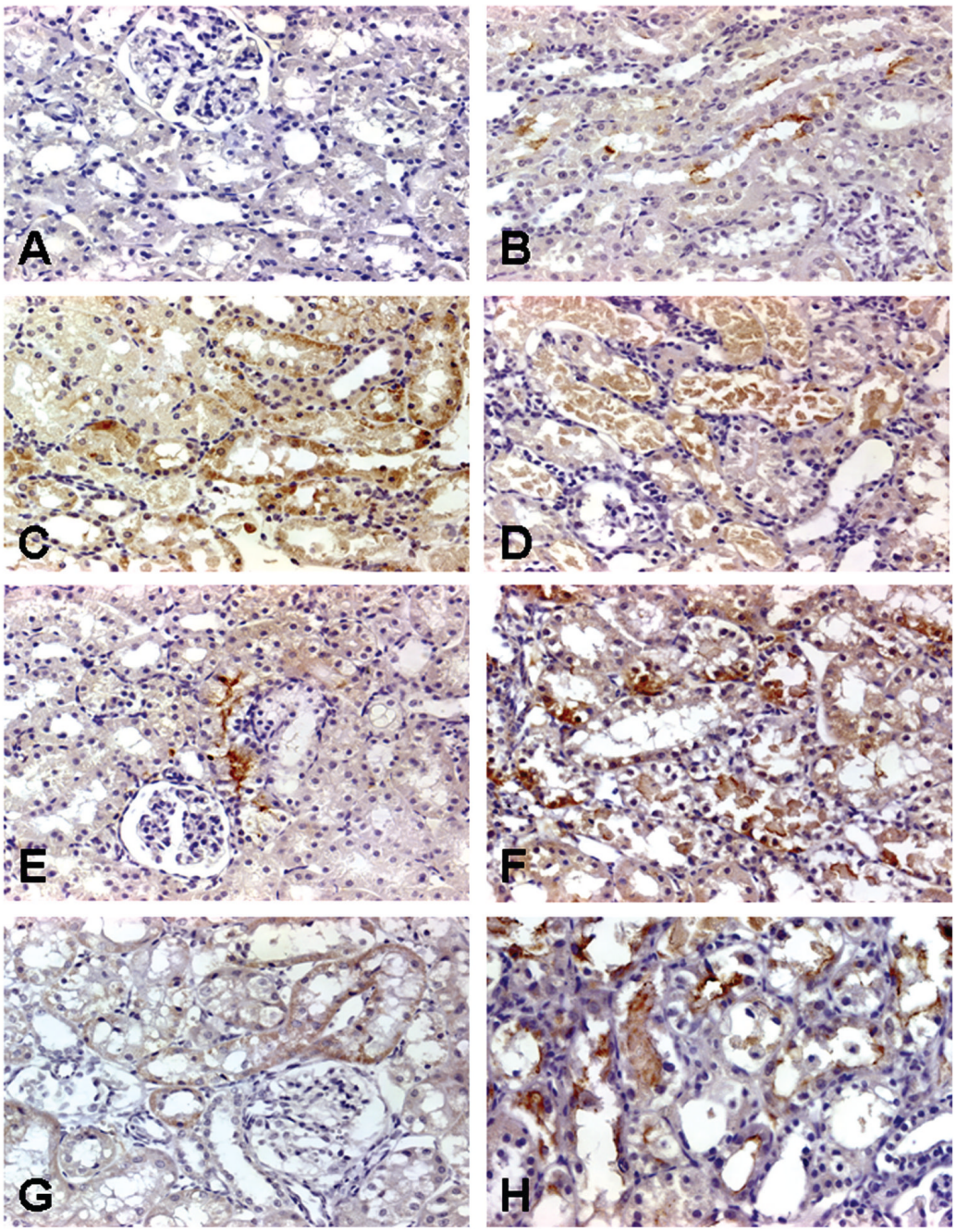

FIGURE 1.

Representative photomicrographs of kidney injury molecule-1 (Kim-1) immunoreactivity in kidneys of rats treated with nephrotoxicants. No Kim-1 expression was found in the cytoplasm of epithelial cells of all segments in the cortex in rats treated with dH_20 vehicle (A). In the time course study with gentamicin (Gen), Kim-1 expression was detected on the surface of epithelial cells in the S1/S2 segments in rats 24 hours after the 3rd daily injection of 100 mg Gen/kg, sc (B). Kim-1 expression was also seen in the cytoplasm of necrotic and dying epithelial cells in the S1/S2 segments in rats 72 hours after the 3rd daily injection of Gen 100 mg/kg, sc (C). Kim-1 was observed in the cytoplasm of desquamated necrotic cells in the lumen of these segments 24 hours after the 3rd injection of Gen 300 mg/kg (D). In the time course studies

with mercury (Hg) or chromium (Cr), Kim-1 expression was detected in rats treated with Hg 0.25 mg/kg, iv, after 24 hours (E) and 72 hours (F) or Cr 5 mg/kg after 24 hours (G) and 72 hours (H). Original magnification of all figures: ×400.

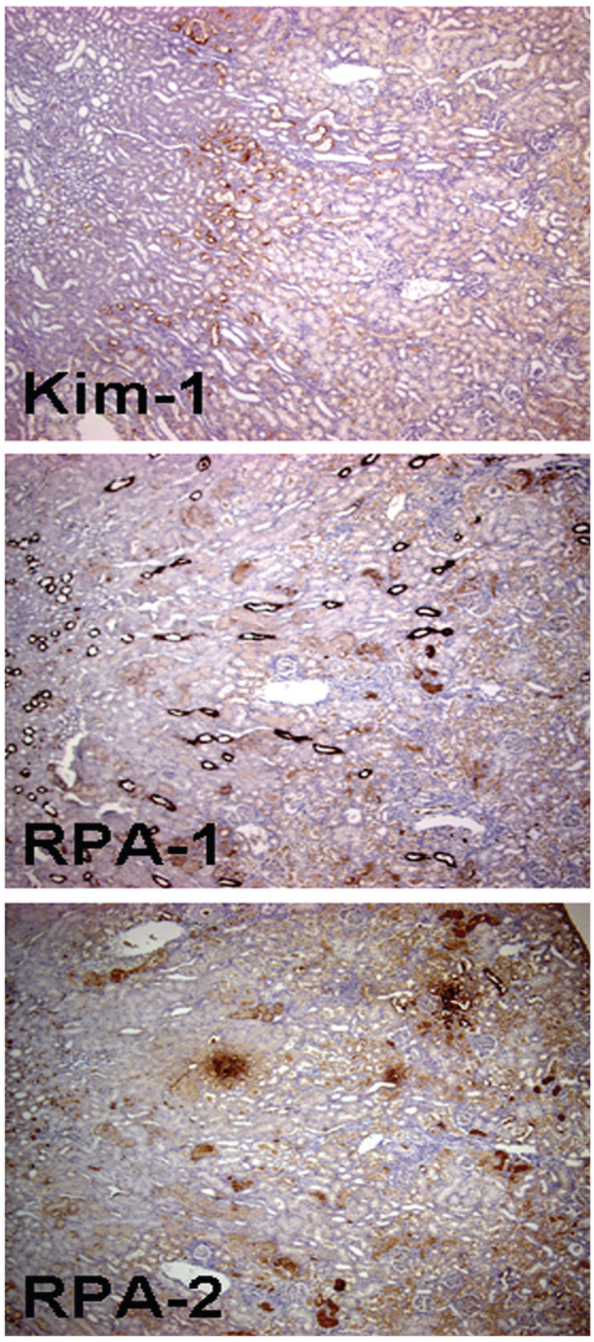

FIGURE 2.
Representative low-magnification photomicrographs showing a higher level of kidney injury molecule-1, renal papillary antigen-1 (RPA-1), and renal papillary antigen-2 (RPA-2) expression in the S1/S2 segments of the nephron when compared with S3 segments in rats 72 hours after the 3rd daily dose of gentamicin 100 mg/kg, sc. Note: RPA-1 expression in collecting ducts and RPA-2 expression in loop of Henle are also visible but are comparable to their respective counterparts in control rats. Original magnification of all figures: ×50.

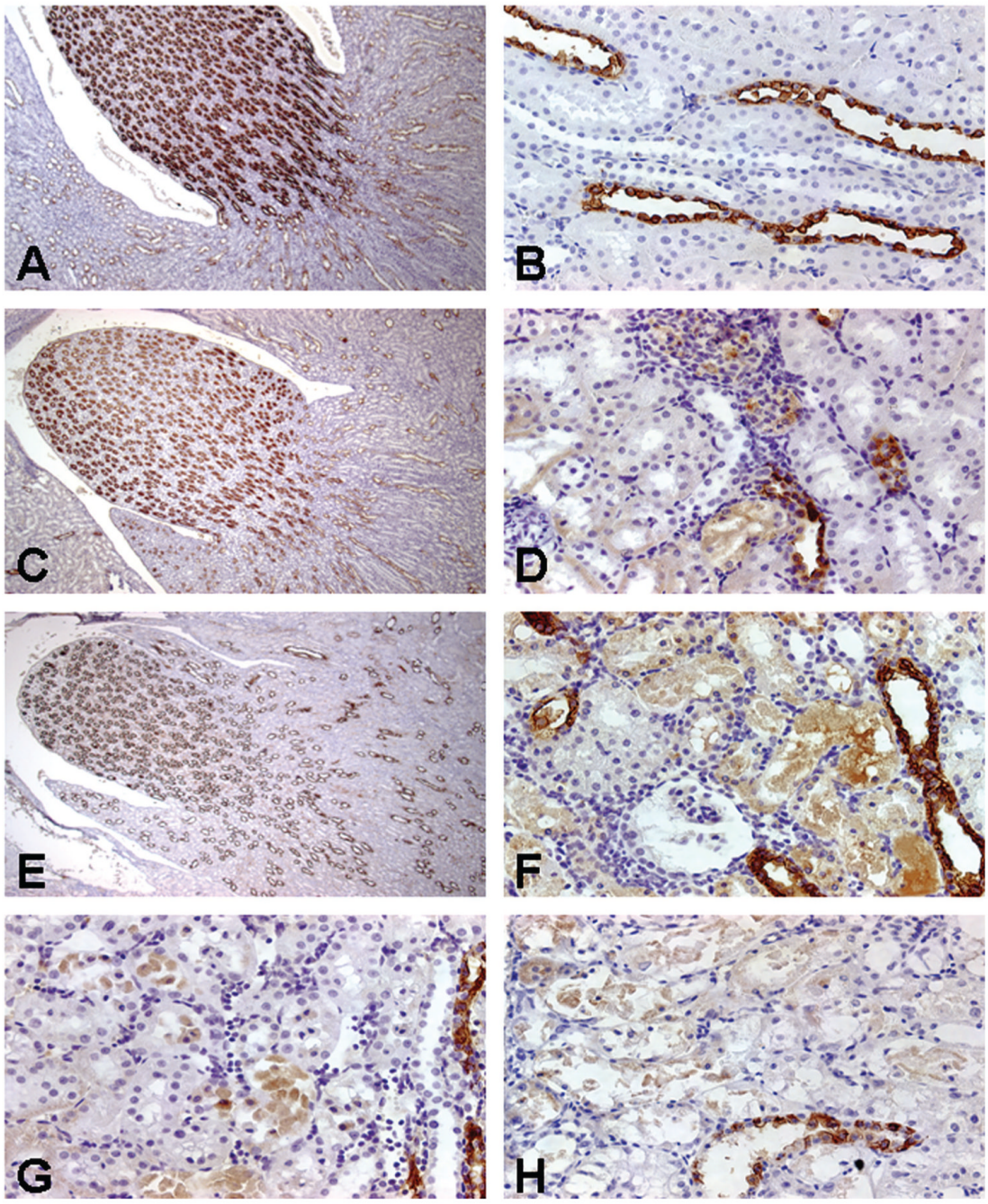

FIGURE 3.

Representative photomicrographs of renal papillary antigen-1 (RPA-1) immunoreactivity in kidneys of rats treated with nephrotoxicants. RPA-1 expression was located predominantly in the medullary collecting duct (CD) epithelial cells (A) and sporadically in the cortical CD epithelial cells (B) in rats treated with saline, iv, for 24 hours. Treatment of rats with gentamicin (Gen) 50 mg/kg, sc, daily for 3 days did not change RPA-1 expression in the medullary CD epithelial cells (C), but RPA-1 appeared in proximal tubular epithelial cells (D). Treatment of rats with high doses of Gen, 300 mg, kg sc, daily for 3 days did not induce significant changes in medullary RPA-1 expression (E), but did result in enhanced S1/S2 segment expression (F). Rats treated with mercury 0.25 mg/kg, iv, for 24 hours expressed RPA-1 in the S3 segments

(G). RPA-1 expression was noted in the S1/S2 segments in rats treated with chromium 5 mg/kg, sc, for 24 hours (H). Original magnification of all figures: ×400, except figures (A, C, E): ×50.

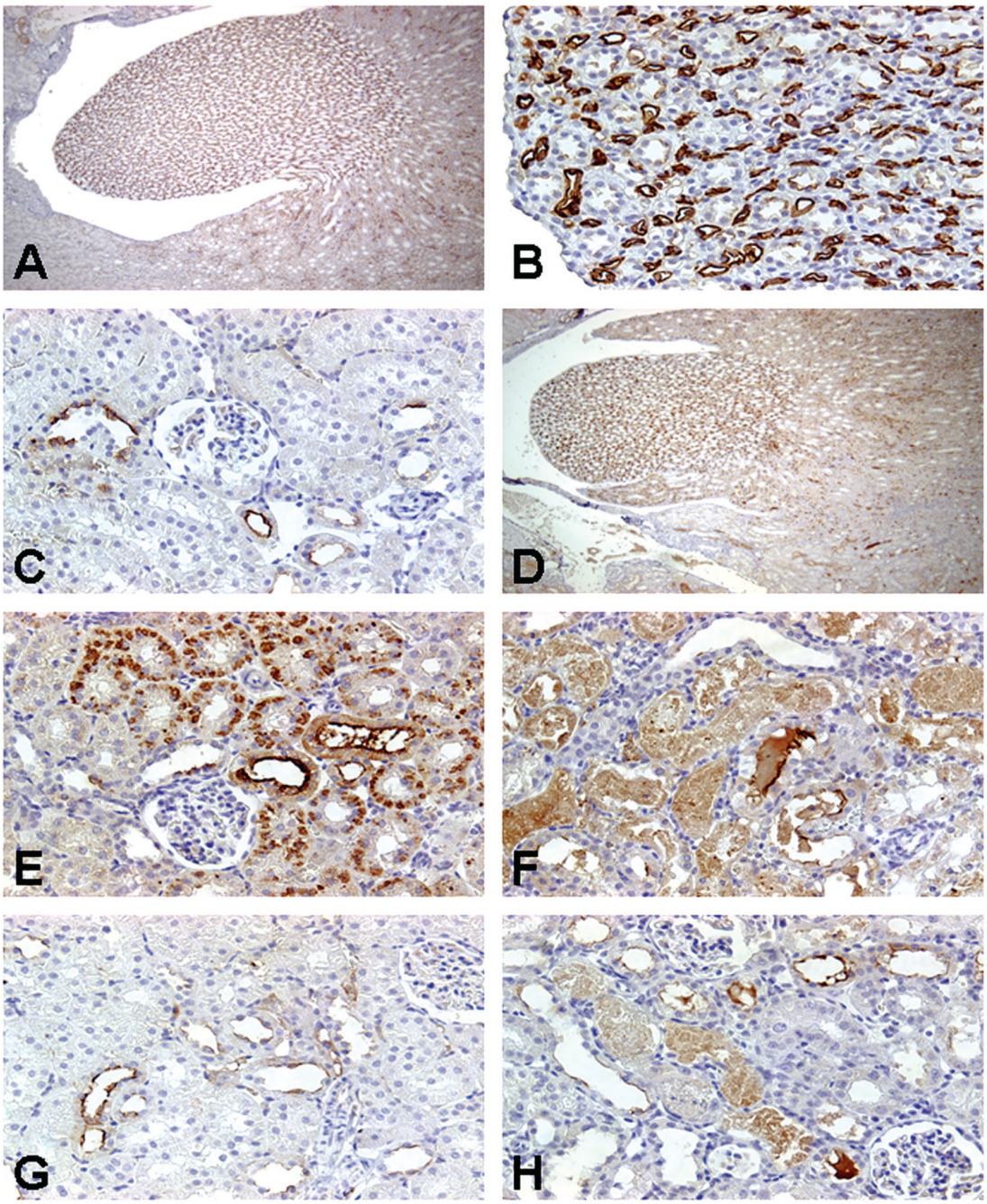

FIGURE 4.

Representative photomicrographs of renal papillary antigen-2 (RPA-2) immunoreactivity in kidneys of rats treated with nephrotoxicants. RPA-2 expression was located predominantly in the epithelial cells of the descending and ascending thin loop of Henle (LH) segments in the medulla (A) in control rats. The immunostaining for RPA-2 in control rats showed homogenous reaction within the cytoplasm of LH cells and intense reaction on their surfaces (B). Note the epithelial cells of medullary collecting ducts in the vicinity of RPA-2-expressing tubules were completely negative. RPA-2 expression was sporadic in the epithelial cells in the ascending thick LH segments of the cortex in control rats (C). Treatment of rats with gentamicin 100 mg/kg, sc, for 3 days did not change RPA-2 expression in the epithelial cells of the descending

and ascending thin LH segments in the medulla (D) but resulted in new expression of RPA-2 in proximal tubular epithelial cells 24 hours (E) and 72 hours (F) after the last dose. There was no RPA-2 expression in the S1/S2 segments in mercury-treated rats (G). In contrast, RPA-2 expression was noted in the S1/S2 segments in chromium-treated rats (H). Original magnification of all figures: ×400, except figures (A, D, G), ×50.

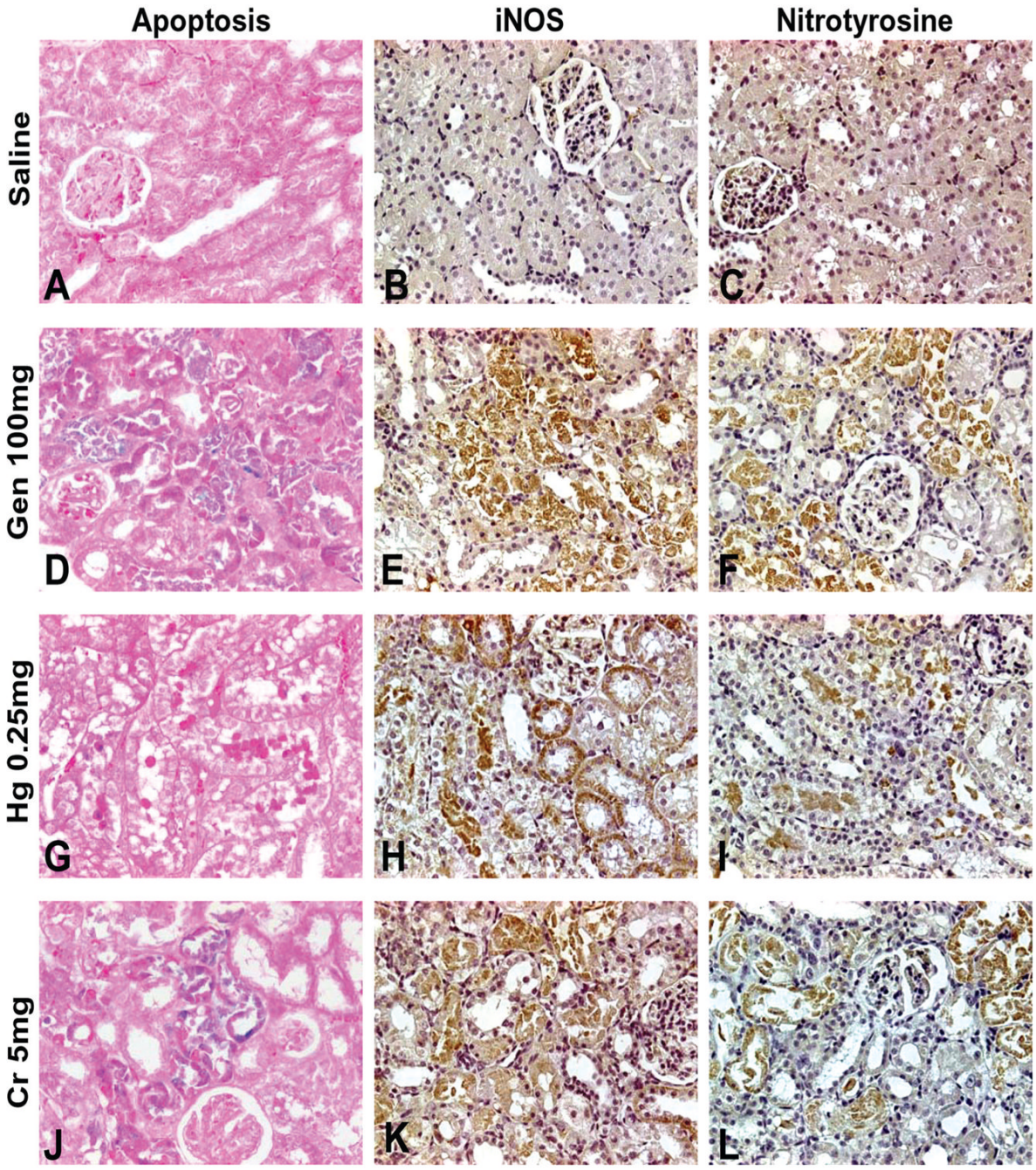

FIGURE 5.

Representative photomicrographs demonstrating immunostaining for apoptosis (A, D, G, J), expression of inducible nitric oxide synthase (iNOS) (B, E, H, K), and expression of nitrotyrosine (C, F, I, L). No immunostaining for apoptosis, iNOS, or nitrotyrosine was observed in saline-treated rats (A-C). Gen- (D-F) and Cr- (J-L) treated rats exhibited immunostaining for apoptosis, iNOS, and nitrotyrosine largely in the S1/S2 segments and to a lesser degree in the S3 segments, whereas Hg- (G-I) treated rats exhibited increased immunostaining for apoptosis, iNOS, and nitrotyrosine almost exclusively in the S3 segments. Apoptosis is indicated by blue color of nuclei. Original magnification of all figures: ×400.

Table 1

Immunolocalization of kidney injury molecule-1 in the kidney of rats, mice, and humans.

Animal species & human	Pathological diagnosis	Immunolocalization	Antibody	References
SD rats	Ischemic reperfusion injury	S3 segments	Rabbit pAb R9	Ichimura et al., 1998
SD rats	TFEC-, folic acid-, cisplatin-nephrotoxicity	S3 segments	Rabbit pAb R9	Ichimura et al., 2004
SD rats	Cisplatin-nephrotoxicity	S3 segments	Rabbit pAb R9	Amin et al., 2004
Wistar rats	Protein-overload nephrotoxicity	Proximal tubular cells of outer medulla	Rabbit pAb R9	van Timmerren et al., 2006
SD rats	Cisplatin-nephrotoxicity	S3 segments	Mouse mAb MARKE-1, -2, -Trap	Vaidya et al., 2006
Ren2 rats	Tubulointerstitial fibrosis	Proximal tubular epithelial cells of cortex	Rabbit pAb R9	de Borst et al., 2007
PKD2 $^{WS25/-}$mice	Polycystic kidney disease	Cyst-lining epithelium derived from proximal tubules and CD	Mouse pAb R9	Kuehn et al., 2002
Human	Acute tubular necrosis	S1/S2 segments	mAb AKG7	Han et al., 2002
Human	Acute tubular injury in human renal transplants	Proximal tubules	mAb AKG7	Zhang et al., 2008
Human	Acute tubular necrosis adjacent to cancer	Proximal tubules	mAb ABE3	Lin et al., 2007
Human	Fibrosis and inflammation	Proximal tubules	mAb AKG7	van Timmerren et al., 2007

pAb R9 = rabbit anti-rat Kim-1 R9 pAb; mAb ABE3, or AKG7 = anti-human hKim-1 mAb; mAb MARKE-1, -2, -Trap = mouse anti-rat Kim-1 ectodomain (MARKE) mAbs.

Table 2

Immunolocalization of Kim-1, RPA-1, RPA-2, iNOS, nitrotyrosine, and apoptosis in Gen-, Hg-, or Cr-treated rats (time response study).

Treatment[a] (mg/kg)	Time[b] (hr)	Renal lesions scores	Apoptosis and related markers in S1-S3 segments			Immunolocalization of Kim-1, RPA-1, and RPA-2				
			Apo	NT	iNOS	Kim-1	RPA-1 (CD)	RPA-1	RPA-2 (LH)	RPA-2
Saline, sc	24	0	—	—	—	—	Positive	—	Positive	—
Gen 100, sc	24	1.5*	++	++	++	++ (S1-S3)	Positive	—	Positive	++ (S1-S3)
Gen 100, sc	72	3.3*	+++	+++	+++	+++ (S1-S3)	Positive	+++ (S1-S3)	Positive	+++ (S1-S3)
Hg 0.25, iv	24	3.0*	++	++	++	++ (S3)	Positive	++ (S3)	Positive	++ (S3)
Hg 0.25, iv	72	3.8*	+++	+++	+++	+++ (S3)	Positive	+ (S3)	Positive	+++ (S3)
Cr 5, sc	24	2.8*	++	++	++	++ (S1-S3)	Positive	+ (S1-S3)	Positive	++ (S1-S3)
Cr 5, sc	72	4.8*	+++	+++	+++	+++ (S1-S3)	Positive	+++ (S1-S3)	Positive	+++ (S1-S3)

IHC keys: −, +, ++, and +++ represent no positive reaction, weak, moderate, and strong positive reaction, respectively. Apo = apoptosis; NT = nitrotyrosine; iNOS = inducible nitric oxide synthase; Kim-1 = kidney injury molecule-1; RPA = renal papillary antigen; CD = collecting ducts; LH = loops of Henle.

*Statistically significantly different when compared with rats treated with saline ($p < .05$).

[a]Treatments: Rats received Gen (100 mg/kg, sc) injected daily for 3 days, or a single injection of mercury (Hg) (0.25 mg/kg, iv) or chromium (Cr) (5 mg/kg, sc).

[b]Rats were euthanized and tissues examined 24 hours or 72 hours after the third injection of Gen or the single injection of Hg or Cr.

Table 3

Immunolocalization of Kim-1 and RPA-1 in Gen-treated rats (dose-response study).

Treatment (mg/kg, sc)	Time[a] (hr)	Renal lesions scores	Immunolocalization of Kim1 and RPA-1		
			Kim-1 (S1-S3 segments)**	RPA-1 (cortical & papillary CD)	RPA-1 (S1-S3 segments)**
dH_2O	24	0.2	—	Positive	—
Gen 50	24	1.2	+	Positive	+
Gen 100	24	1.5*	+	Positive	+
Gen 150	24	2.3*	++	Positive	+
Gen 200	24	3.5*	+++	Positive	++
Gen 300	24	4.8*	++++	Positive	+++

Kim-1 = kidney injury molecule-1; RPA = renal papillary antigen; Gen = gentamicin sulfate; CD = collecting ducts.

*Statistically significantly different when compared with rats treated with saline ($p < .05$).

**The expression of Kim-1 and RPA-1 is greatest in the S1/S2 segments.

[a]Rats were euthanized and tissues examined 24 hours after the third daily injection of Gen.